THE JOURNAL OF PHYSICAL CHEMISTRY Letters

Letter

pubs.acs.org/JPCL

A Fresh Look at Resonances and Complex Absorbing Potentials: Density Matrix-Based Approach

Thomas-C. Jagau,*[,†] Dmitry Zuev,[†] Ksenia B. Bravaya,[‡] Evgeny Epifanovsky,[†,§,∥] and Anna I. Krylov[†]

[†]Department of Chemistry, University of Southern California, Los Angeles, California 90089-0482, United States

[‡]Department of Chemistry, Boston University, Boston, Massachusetts 02215-2521, United States

[§]Department of Chemistry, University of California, Berkeley, California 94720, United States

[∥]Q-Chem Inc., 6601 Owens Drive, Suite 105, Pleasanton, California 94588, United States

Supporting Information

ABSTRACT: A new strategy of using complex absorbing potentials (CAPs) within electronic structure calculations of metastable electronic states, which are ubiquitous in chemistry and physics, is presented. The stumbling block in numerical applications of CAPs is the necessity to optimize the CAP strength for each system, state, and one-electron basis set, while there is no clear metric to assess the quality of the results and no simple algorithm of achieving numerical convergence. By analyzing the behavior of resonance wave functions, we found that robust results can be obtained when considering fully stabilized resonance states characterized by constant density at large η (parameter determining the CAP strength). Then the perturbation due to the finite-strength CAP can be removed by a simple energy correction derived from energy decomposition analysis and response theory. The utility of this approach is illustrated by CAP-augmented calculations of several shape resonances using EOM-EA-CCSD with standard Gaussian basis sets.

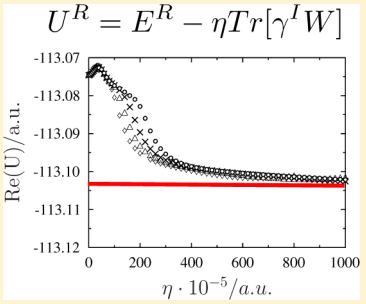

SECTION: Spectroscopy, Photochemistry, and Excited States

Metastable electronic states are important in diverse areas of science and technology ranging from high-energy applications (plasmas, attosecond and X-ray spectroscopies) to electron−molecule collisions (interstellar chemistry, radiolysis, DNA damage by slow electrons). The description of processes involving resonances is not complete if the finite lifetime of the metastable states is not taken into account. For an example illustrating the importance of resonances in biomolecules and difficulties in their theoretical description as well as in interpretation of experimental data, consider *p*-coumaric acid,[1−3] a model chromophore for the photoactive yellow protein, whose bright excited state is metastable in the gas phase.

From the quantum mechanical point of view, such states belong to the continuum part of the spectrum, and, therefore, their wave functions are not L^2-integrable, which makes their calculation by standard electronic structure techniques difficult. A number of approaches based on complex coordinates/potentials that circumvent the need to work with the continuum functions (or deal with boundary conditions) have been proposed.[4−6] The most straightforward approach, the so-called complex-scaling formalism, has rigorous theoretical justification,[7] however, its application to molecular systems is complicated by numerical (extreme basis-set sensitivity) as well as conceptual (separation of nuclear and electronic motions) issues.

These problems are avoided in an alternative approach in which the original (nonscaled) Hamiltonian is augmented by a complex potential $-i\eta\hat{W}$ devised to absorb the diverging tail of the resonance wave function (see refs 8−10 and references therein for a historic perspective). These complex absorbing potential (CAP) methods are related to exterior complex scaling methods[11,12] and, under certain conditions, one can extract exact resonance positions (E_{res}) and widths (Γ) from CAP-based calculations.[8−10,13−15] Unfortunately, straightforward inclusion of a simple CAP (e.g., harmonic potential with an onset at $|r| = r^0$) in an electronic structure calculation may lead to unacceptable perturbations of the resonance wave functions and, consequently, energies. Moreover, the results are quite sensitive to the CAP onset and one-electron basis set.

CAPs were first applied within time-dependent calculations[16] and, historically, the perturbations due to the CAP have been called reflections. These reflections by CAPs have been analyzed in detail in refs 13 and 15 using semiclassical techniques, the main results being that a reflection-free CAP should be energy dependent (as the reflection probability depends on the energy) and that the finite-basis set representation of the CAP may lead to additional reflections, which explains the nature of the sensitivity of CAP-based calculations to the one-electron basis set and the CAP box size (the onset of the CAP).

Received: November 17, 2013
Accepted: December 26, 2013
Published: December 26, 2013

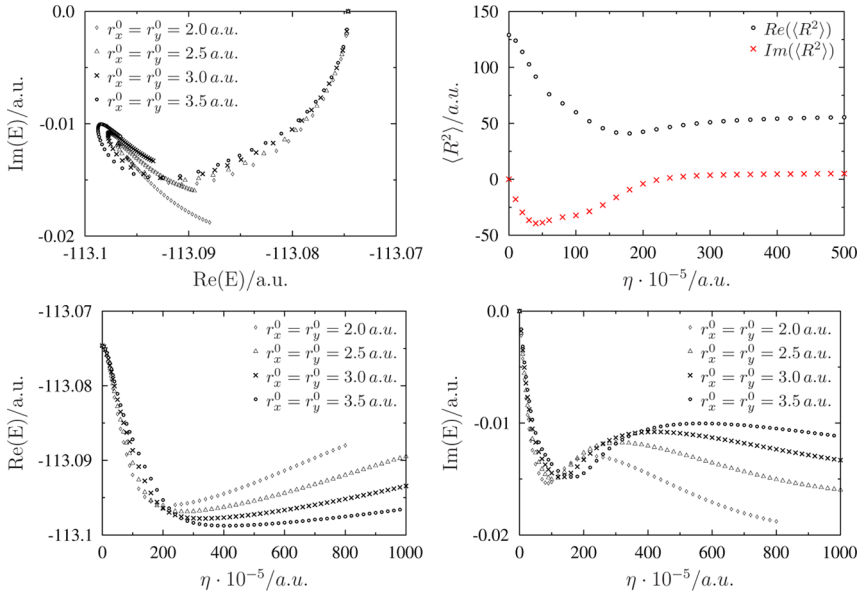

Figure 1. $^2\Pi$ shape resonance in CO^- computed by EOM-EA-CCSD/aug-cc-pVTZ+3s3p with CAP. Top left: $E(\eta)$ for several box sizes (r_z^0 = 5 bohr). Top right: Real and imaginary part of $\langle R^2\rangle$ of the resonance wave function. Bottom: $E^R(\eta)$ and $E^I(\eta)$.

Another important conclusion from early CAP studies[8] was that there is an optimal CAP strength (when CAP is used in finite bases). In the complete basis set limit, the energy of the resonance is obtained by $\eta \to 0$, however, in the finite basis set in which $\hat{W}$ is cut off at a certain distance, one needs to work with finite η sufficient to stabilize the resonance. Consequently, when the CAP is too weak (η is too small), the resonance is not stabilized and its energy depends strongly on the CAP strength. When the CAP is too strong, the reflections affect the resonance significantly, thereby spoiling the resonance energy. Thus, there is an optimal value of the CAP strength, η_{opt}, which is system- and state-dependent. As a practical recipe of choosing η_{opt}, it was suggested[13] that one can determine an optimal CAP strength by analyzing η-trajectories, $E(\eta)$, and identifying the η-value around which the trajectories slow down, leading to the following condition:

$$\left|\eta \frac{dE}{d\eta}\right| \approx 0 \tag{1}$$

This energy-based criterion, eq 1, has been employed in most CAP studies (see, for example, recent CAP applications[17−19]).

The problems with such straightforward CAP calculations are clearly illustrated by the results for resonance states of N_2^-, CO^-, and Be^- compiled in the Supporting Information (SI). First, the shape of the trajectories is rather different for different systems; often, the extremum is not very prominent. Second, the results are quite sensitive to the box size (and the basis set): Variations of 0.2 eV are observed in E_{res} and Γ even for relatively small variations of the box size (Table S1). Third, the numerical analysis of the derivative shows that the condition from eq 1 is not quite satisfied — and it is unclear what value of the derivative is acceptable. Finally, the stabilization of the trajectories is observed at rather different values of η, which makes it unclear in which range η should be varied for each particular system (and state, and box size) and, in cases when stabilization is achieved at large η, whether the result is strongly perturbed by the CAP.

Here we present a new strategy of exploiting CAPs within electronic structure calculations. Based on energy decomposition analysis and response theory, we introduce a simple formula for deperturbing the resonance position and width and an alternative criterion for finding an optimal value of η. Physically, our approach is grounded in the behavior of the resonance wave function and, ultimately, the one-particle density matrix. We show that when the CAP is sufficiently strong, both real and imaginary parts of the density become near-stationary (showing that the resonance is stabilized). Then the perturbation to the resonance position by the CAP can be eliminated by removing the energy component due to the imaginary part of the density. The imaginary density arises due to reflections; thus, removing these terms removes the effect of reflections. A similar correction is introduced for the resonance width. The optimal η is found by considering the deperturbed resonance energies; moreover, we argue that η_{opt} is not the same for real and imaginary parts. Our approach results in a computationally more robust scheme in which the dependence on the box size is significantly reduced and leads to good numeric results.

The results were obtained with a new code extending our implementation of complex-scaled EOM-CC methods[20] to include CAPs. The code utilizes a general-purpose tensor library[21] and is implemented within Q-Chem.[22] The details of the implementation will be reported in an upcoming paper; here we focus on new insights into the CAP technique. In short, in our implementation, the harmonic CAP is added to the original Hamiltonian H:

$$\hat{H}(\eta) = \hat{H} - i\eta\hat{W} \tag{2}$$

$$\hat{W} = 0 \text{ if } |r_\alpha| < r_\alpha^0 \tag{3}$$

$$=(r_\alpha - r_\alpha^0)^2 \text{ if } |r_\alpha| > r_\alpha^0 \tag{4}$$

where r_α denotes the three Cartesian coordinates (α = x,y,z). Thus, the CAP is characterized by the strength η and the box parameters, r_x^0, r_y^0, and r_z^0. The Hartree−Fock, CCSD, and EOM-CCSD equations are solved for the CAP-augmented Hamiltonian using the c-product.[5,23] Thus, the MO coefficient matrix C, the coupled-cluster amplitudes T, and the EOM-CC

dx.doi.org/10.1021/jz402482a | J. Phys. Chem. Lett. 2014, 5, 310−315

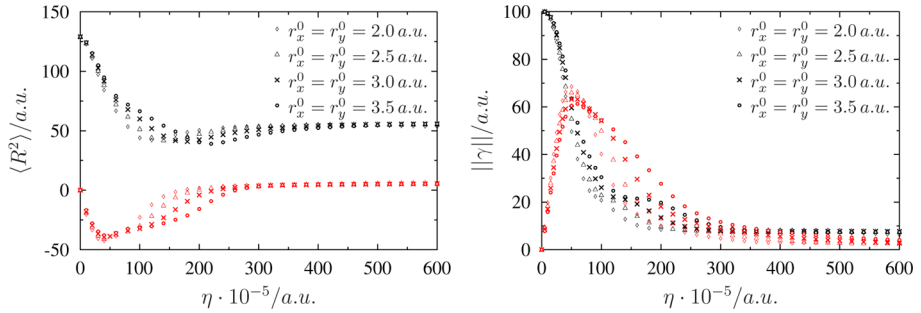

Figure 2. Real (black) and imaginary (red) parts of the expectation value $\langle R^2\rangle$ (left) and the Frobenius norm of γ (right) for the $^2\Pi$ shape resonance in CO^- computed by CAP-augmented EOM-EA-CCSD/aug-cc-pVTZ+3s3p.

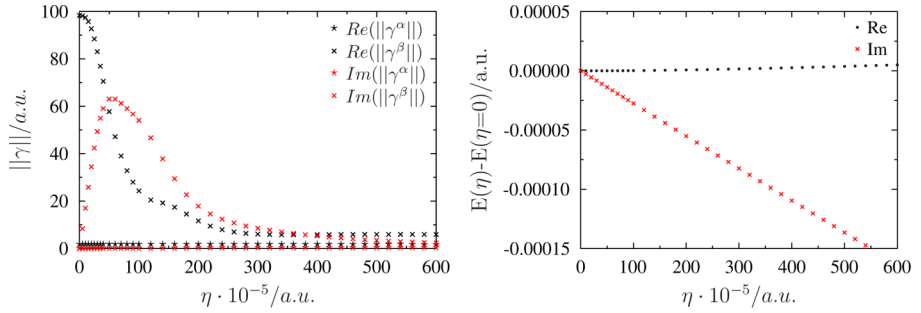

Figure 3. Left: Real and imaginary parts of the Frobenius norm of the α and β parts of γ (the spin of the extra electron is β). Right: Deviation of the real and imaginary parts of the ground-state energy from the respective unperturbed values. Box size: $r_x^0 = r_y^0 = 3$ bohr and $r_z^0 = 5$ bohr.

amplitudes R are complex. The matrices of the one-particle and two-particle parts of the initial Hamiltonian, h and II, as well as W, are real in the AO basis; however, they become complex-symmetric in the MO basis. Since the focus of this paper is on shape resonances obtained by electron attachment to closed-shell species, we employ EOM-EA-CCSD (EOM-CCSD for electron attachment) in which the reference wave function corresponds to an N-electron closed-shell system and the resonance (N+1-electron) state is described by EOM-EA operators.[24]

Figure 1 shows the results for the $^2\Pi$ resonance in CO^- computed using various box sizes (see SI for details about geometry and basis set). The size of the reference wave function in these calculations is $(\langle X^2\rangle)^{1/2} = (\langle Y^2\rangle)^{1/2} = 2.76$ bohr and $(\langle Z^2\rangle)^{1/2} = 4.97$ bohr ($(\langle R^2\rangle)^{1/2} = 6.33$ bohr); we use these values as a rough estimate of the CAP box size. All $E(\eta)$ trajectories have similar shape; however, η_{opt} and $E(\eta_{opt})$ vary significantly (~0.2 eV) with the box size (see SI, Table S1). We also note that the values of the derivatives, $(dE/d\eta)_{\eta=\eta_{opt}}$ and $(\eta(dE/d\eta))_{\eta=\eta_{opt}}$, are not exactly zero ($\approx 10^{-3}$ a.u. for CO^-). Furthermore, we do not observe any correlation between the smallness of the derivative and the quality of the computed resonance position and width. In sum, short of comparing against the experimental value, there is no clear way to judge the quality of the results.

Figure 1b shows the dependence of the spatial extent of the resonance wave function as a function of η ($|\langle R^2\rangle|$ is not shown as it follows the real part very closely). We observe that, as the strength of the CAP increases, the wave function shrinks. Interestingly, after a certain value of η, $\langle R^2\rangle$ remains more or less constant (the asymptotic value of $(\langle R^2\rangle)^{1/2}$ is about 7.1 bohr, which is only slightly larger than that of the reference state). This behavior illustrates the stabilization of the resonance by the CAP. Even more interesting is the behavior of the real and imaginary parts of $\langle R^2\rangle$: While the real part decreases at small η, the imaginary part exhibits a non-monotonous behavior before reaching an asymptote. Unlike $E(\eta)$ trajectories that have very different shapes in different systems, the behavior of the resonance wave function appears to be similar in all systems that we considered.

We note that the asymptotic value of the imaginary part is close to zero. In the usual metric of the standard scalar product, it is only the imaginary part of the wave function that could give rise to the current density:

$$\langle\Psi|\hat{j}|\Psi\rangle = -\frac{i}{2}(\langle\Psi|\nabla\Psi\rangle - \langle\nabla\Psi|\Psi\rangle) = Im(\langle\Psi|\nabla\Psi\rangle) = Tr[\nabla\gamma^I] \quad (5)$$

where γ^I is the imaginary part of the one-particle density matrix. Thus, for a perfectly stabilized (but unperturbed) resonance, one should expect no current and, therefore, $\gamma^I = 0$. The nonzero γ^I in the asymptotic region manifests the reflections by the CAP. As will be shown below, γ^I is the leading contribution to the perturbation by the CAP.

The bottom part of Figure 1 shows the behavior of the real and imaginary parts of the resonance energy as a function of η. We note that $E^R(\eta)$ exhibits a minimum, whereas $E^I(\eta)$ has two extrema. Asymptotically, both $E^R(\eta)$ and $E^I(\eta)$ exhibit a linear behavior, with the slope depending on the box size. As will be shown below by energy decomposition analysis, this behavior is due to the asymptotic nearly constant behavior of the resonance density.

In order to make connections between the properties of the resonance wave function such as $\langle R^2\rangle$ and its energy, it is useful to employ the following relationship based on the Cauchy–Schwarz inequality:

$$|\langle\Psi|\hat{A}|\Psi\rangle| = |Tr[A\gamma]| \leq \|A\|\cdot\|\gamma\| \quad (6)$$

dx.doi.org/10.1021/jz402482a | J. Phys. Chem. Lett. 2014, 5, 310−315

Table 1. Resonance Positions and Widths, in eV, for Selected Systems Computed by EOM-EA-CCSD/aug-cc-pVTZ+3s3p[a]

system	box parameters r_α^0	$\|\|W\|\|$	η_{opt}	η'_{opt}	E_{res}/eV	Γ/eV
CO^-						
	2.0/2.0/5.0	592.3	0.0066	0.0046	1.979	0.468
	2.5/2.5/5.0	533.2	0.0084	0.0058	1.968	0.456
	3.0/3.0/5.0	480.7	0.0110	0.0076	1.954	0.433
	3.5/3.5/5.0	434.2	0.0155	0.0100	1.937	0.406
	4.0/4.0/5.0	393.2	0.0210	0.0135	1.916	0.380
	experiment				1.50	0.40
N_2^-						
	2.5/2.5/3.5	528.9	0.0047	0.0093	2.579	0.216
	2.76/2.76/4.88	454.8	0.0063	0.0129	2.571	0.213
	3.5/3.5/4.5	398.0	0.0086	0.0194	2.564	0.180
	experiment				2.32	0.41
Be^-						
	2.0/2.0/2.0	3156.9	0.0010	0.0038	0.807	0.058
	4.0/4.0/4.0	2579.5	0.0025	0.0067	0.801	0.129
	6.0/6.0/6.0	2099.3	0.0067	0.0110	0.794	0.116

[a]Box sizes, $\|\|W\|\|$, and optimal values of η for real and imaginary parts (η_{opt} and η'_{opt}) are also shown (all in atomic units). The size of the reference wave functions is $(\langle X^2\rangle)^{1/2} = (\langle Y^2\rangle)^{1/2} = 2.76$ bohr, $(\langle Z^2\rangle)^{1/2} = 4.97$ bohr for CO, $(\langle X^2\rangle)^{1/2} = (\langle Y^2\rangle)^{1/2} = 2.76$ bohr, $(\langle Z^2\rangle)^{1/2} = 4.88$ bohr for N_2, and $(\langle X^2\rangle)^{1/2} = (\langle Y^2\rangle)^{1/2} = (\langle Z^2\rangle)^{1/2} = 2.34$ bohr for Be.

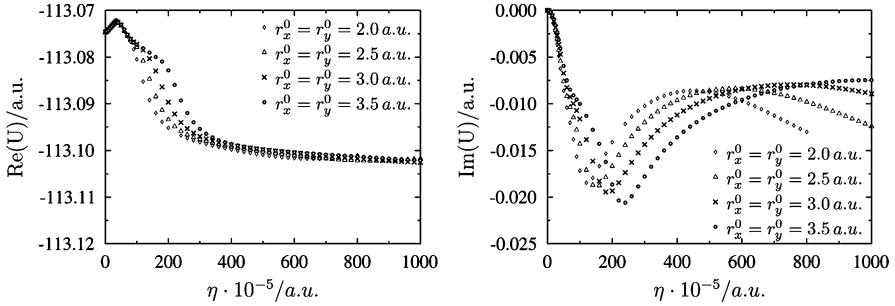

Figure 4. U^R (left) and U^I (right) for the $^2\Pi$ shape resonance in CO^- computed by CAP-augmented EOM-EA-CCSD/aug-cc-pVTZ+3s3p.

where γ is a reduced one-particle density matrix:

$$\gamma_{pq} = (\Psi|p^+q|\Psi) \tag{7}$$

$\hat{A}$ is a one-particle operator, and A is its matrix representation in a one-electron basis. Consistent with the calculation of the energy and amplitudes, the density matrices are defined using the c-product, i.e., the bra state in eq 7 is not complex conjugated. Equation 6, which has been recently introduced to evaluate trends in nonadiabatic couplings,[25] shows that the magnitude of an expectation value of a one-particle operator is proportional to (or, more accurately, symbatic with) the norm of the respective one-particle density matrix, $\|\gamma\|$. This is illustrated in Figure 2 that shows $\langle R^2\rangle$ and $\|\gamma\|$. A similar inequality can be applied for the one-particle part of the resonance energy. Thus, trends in $\|\gamma\|$ determine the behavior of $\langle R^2\rangle$ and E.

The analysis of the α and β parts of γ (shown in Figure 3) reveals that the trends in γ (and, consequently, $\langle R^2\rangle$) are dominated by the excess electron — while the β-part of γ shows strong variations with η, the α-part remains constant (the spin of the excess electron is β). The latter is encouraging as it illustrates that the "core" electrons are not strongly perturbed by the CAP. This is consistent with the observed small changes in the reference energy shown in Figure 3.

To proceed further, we write down an expression for the total energy using one and two-particle density matrices, γ and Γ:

$$E = \sum_{\mu\nu} \gamma_{\mu\nu} f_{\mu\nu} + \sum_{\mu\nu\sigma\rho} \Gamma_{\mu\sigma\nu\rho} \langle \mu\sigma \| \nu\rho \rangle = Tr[\gamma f] + Tr[\Gamma II] \tag{8}$$

where all matrices are represented in the AO basis. The real and imaginary contributions are thus:

$$E^R = Tr[\gamma^R f] + Tr[\Gamma^R II] + \eta Tr[\gamma^I W]$$
$$E^I = Tr[\gamma^I f] + Tr[\Gamma^I II] - \eta Tr[\gamma^R W] \tag{9}$$

We note that the explicit dependence of the energy on η (and on W) is linear, both for E^R and E^I. There is, however, also an implicit dependence, as the wave function amplitudes (and, consequently, the density matrices) depend on η. The explicit dependence on η explains the asymptotic behavior of E^R and E^I. Since asymptotically γ^I and γ^R are approximately constant (as illustrated in Figure 2), the energy is proportional to η. The slope is determined by $Tr[\gamma^I W]$ which, in turn, is proportional to $\|W\|$ by virtue of eq 6. The value of $\|W\|$ depends on the basis set representation of W. When using the same finite one-electron basis set, $\|W\|$ depends on the CAP box size and the use of larger boxes results in smaller $\|W\|$ due to incomplete representation of W (see Table 1).

Based on eq 9, the explicit dependence of the resonance energy on the CAP can be removed by simply subtracting $\eta Tr[\gamma W]$ from the resonance energy. One can consider this correction as the first-order correction accounting for the perturbation due to the finite CAP strength. Thus, instead of

dx.doi.org/10.1021/jz402482a | J. Phys. Chem. Lett. 2014, 5, 310−315

looking at raw resonance energies (as commonly done in CAP calculations[17−19]), we propose to consider the first-order corrected (i.e., deperturbed) quantities:

$$U^R = E^R - \eta Tr[\gamma^I W] \tag{10}$$

$$U^I = E^I + \eta Tr[\gamma^R W] \tag{11}$$

The dependence of the resonance energy on η has also been analyzed in ref 8 using Taylor series, where it was also noted that the linear part can be described as an expectation value of $\hat{W}$ with respect to the resonance wave function. Our correction is nearly identical to the first-order correction proposed in ref 8, except that we advocate a different criterion for finding η_{opt} (and this is essential for the method's success).

To better understand the physical meaning of the correction, we note that the η-dependent contribution to the resonance position E^R would be zero if either η or γ^I were zero. Thus, one can describe this term as the perturbation due to the CAP or as a perturbation due to reflections by the CAP. This immediately suggests that E^R can be corrected by simply subtracting this term as done in eq 10.

The deperturbed quantities U^R and U^I are shown in Figure 4 for the $^2\Pi$ resonance state of CO^-. We observe that the dependence on the box size is almost entirely eliminated for $U^R(\eta)$, which asymptotically exhibits nearly constant behavior. Unlike raw $E(\eta)$ trajectories, the deperturbed quantities exhibit similar asymptotic trends in all systems. We define the resonance position (E_{res}) as $U^R(\eta_{opt}) - E_{CC}(\eta = 0)$, where η_{opt} is determined within the region of approximate stationarity by $U^R(\eta) = \min$ and $E_{CC}(\eta = 0)$ is an unperturbed CCSD reference energy. As illustrated by the resonance positions listed in Table 1, the computed values show little variation with the box size and are in good agreement with experiment.

The behavior of $U^I(\eta)$ is more complex, and the region of nearly constant behavior is much smaller, which manifests itself by the maxima at $\eta > 3 \times 10^{-3}$. We attribute this behavior to the terms of second order in η (see below). We determine the resonance width as $\Gamma = 2U^I(\eta'_{opt})$, where η'_{opt} is determined by the location of the maximum in $U^I(\eta)$. The so-computed Γ values show small variations with the box size and, again, reasonable agreement with the experimental values (and other calculations), as illustrated by Table 1 and in the SI (Table S3). It should be noted that for lifetimes, the comparison with the experimental values is not straightforward, in particular, in the case of molecules[26] where nuclear motions should be taken into account. Thus, our focus here is on the stability of the results with respect to the parameters of the calculations rather than on establishing absolute error bars for the approach, which will be pursued in future work.

In sum, using the new approach, the variations in E_{res} and Γ do not exceed 0.09 eV (to be compared with 0.2−0.3 eV when using the original approach). We note that the use of the condition $\eta \cdot dU/d\eta = \min$, similar to eq 1, gives rise to results similar to those listed in Table 1. Also, we add that the criterion $d^2E/d\eta^2 = \min$ proposed in ref 9 leads to almost identical values. However, when using the condition proposed in ref 8, i.e., $\eta Tr[\gamma W] = \min$, the results are almost as poor as in the original approach (SI, Table S2).

To better understand the behavior of the deperturbed energies as well as the rationale for using different η_{opt} values for real and imaginary parts of U, let us analyze in more detail the condition from eq 1. By using EOM-CC response theory, one arrives at the following expression for the gradient $dE/d\eta'$ ($\eta' = \eta - \eta_{opt}$):

$$\left(\frac{dE}{d\eta'}\right)_{\eta'=0} = -iTr[\tilde{\gamma} W] \tag{12}$$

where $\tilde{\gamma}$ is a fully relaxed density matrix that includes amplitudes and orbital relaxation. The real and imaginary parts are

$$\left(\frac{dE}{d\eta'}\right)^R_{\eta'=0} = Tr[\tilde{\gamma}^I W] \tag{13}$$

$$\left(\frac{dE}{d\eta'}\right)^I_{\eta'=0} = -Tr[\tilde{\gamma}^R W] \tag{14}$$

One can easily see that the condition $dE/d\eta = 0$ can only be satisfied for the real part (when $\tilde{\gamma}^I = 0$). However, it is more difficult to satisfy this condition for the imaginary part, as $\tilde{\gamma}^R$ cannot be zero (the only way is to use such a large box that there is no overlap between the real part of the resonance density and W). This is consistent with numerical results for $E(\eta)$ that always show a finite value of the derivative in the special points of the trajectory (see SI).

Finally, the full derivative can be written as

$$\left(\frac{dE}{d\eta}\right)^R = \sum_{\mu\nu}\left(\gamma^I_{\mu\nu} W_{\mu\nu} + \frac{d\gamma^R_{\mu\nu}}{d\eta} f_{\mu\nu} + \frac{d\gamma^I_{\mu\nu}}{d\eta}\eta W_{\mu\nu}\right) + \sum_{\mu\nu\sigma\rho}\frac{d\Gamma^R_{\mu\sigma\nu\rho}}{d\eta}\langle\mu\sigma\|\nu\rho\rangle \tag{15}$$

$$\left(\frac{dE}{d\eta}\right)^I = \sum_{\mu\nu}\left(-\gamma^R_{\mu\nu} W_{\mu\nu} + \frac{d\gamma^I_{\mu\nu}}{d\eta} f_{\mu\nu} - \frac{d\gamma^R_{\mu\nu}}{d\eta}\eta W_{\mu\nu}\right) + \sum_{\mu\nu\sigma\rho}\frac{d\Gamma^I_{\mu\sigma\nu\rho}}{d\eta}\langle\mu\sigma\|\nu\rho\rangle \tag{16}$$

This again shows that there is no simple relationship between $(dE/d\eta)^{R \text{ or } I} = 0$ and $\gamma^{R \text{ or } I} = 0$. We also note that if γ and Γ are constant with respect to η (as we observe in Figure 2), then the derivative is

$$\left(\frac{dE}{d\eta}\right)^R = Tr[\gamma^I W] \tag{17}$$

$$\left(\frac{dE}{d\eta}\right)^I = -Tr[\gamma^R W] \tag{18}$$

which suggests that once η_{opt} is reached, the energies depend linearly on η and the deperturbed quantities should be constant. The observed small variations in U^R and larger variations in U^I suggest that the terms quadratic in η [third terms in eqs 15 and 16] kick in for large η. The different signs of these terms explain why U^R exhibits a (shallow) minimum in the asymptotic region, whereas U^I has a maximum. Thus, evaluating the resonance position and width at points where the first-order corrected quantities exhibit extrema (in the asymptotic region) effectively eliminates the contributions due to the quadratic term.

We note that the two terms depending on $d\gamma/d\eta$ are fundamentally different: One depends on the variations of γ in

dx.doi.org/10.1021/jz402482a | J. Phys. Chem. Lett. 2014, 5, 310−315

the interaction region, whereas the other is governed by the density derivative at large distances, where the CAP is effective.

In summary, we presented a new strategy of computing resonance positions and widths using standard electronic structure methods augmented by CAP. By using first-order corrections, we significantly reduced the dependence of the results on the box size. We observed good numeric performance using moderately augmented standard Gaussian basis sets. Thus, our protocol is much more black-box than the original procedure based on uncorrected η-trajectories. By analyzing the properties of the resonance wave functions, we showed that robust results are obtained when considering fully stabilized resonances (constant density at large η) while correcting for the perturbation due to the CAP. We also made the connection between the energy corrections and removing the reflections due to the CAP.

■ ASSOCIATED CONTENT

Supporting Information

Computational details, $E(\eta)$ trajectories, as well as additional results. This information is available free of charge via the Internet at http://pubs.acs.org.

■ AUTHOR INFORMATION

Notes

The authors declare no competing financial interest.

■ ACKNOWLEDGMENTS

This work is supported by the Army Research Office through the W911NF-12-1-0543 grant. We also acknowledge support from the Humboldt Research Foundation (Bessel Award to A.I.K. and Feodor Lynen fellowship to T.C.J.). We thank Eric Sundstrom for making his general SCF code available and Dr. Yihan Shao (Q-Chem) for his help with the implementation of CAPs.

■ REFERENCES

(1) Gromov, E. V.; Burghardt, I.; Köppel, H.; Cederbaum, L. S. Impact of Sulfur vs Oxygen on the Low-Lying Excited States of *trans-p*-Coumaric Acid and *trans-p*-Coumaric Thio Acid. *J. Phys. Chem. A* **2005**, *109*, 4623−4631.

(2) Rocha-Rinza, T.; Christiansen, O.; Rajput, J.; Gopalan, A.; Rahbek, D. B.; Andersen, L. H.; Bochenkova, A. V.; Granovsky, A. A.; Bravaya, K. B.; Nemukhin, A. V.; et al. Gas Phase Absorption Studies of Photoactive Yellow Protein Chromophore Derivatives. *J. Phys. Chem. A* **2009**, *113*, 9442−9449.

(3) Zuev, D.; Bravaya, K. B.; Crawford, T. D.; Lindh, R.; Krylov, A. I. Electronic Structure of the Two Isomers of the Anionic Form of p-Coumaric Acid Chromophore. *J. Chem. Phys.* **2011**, *134*, 034310.

(4) Reinhardt, W. P. Complex Coordinates in the Theory of Atomic and Molecular Structure and Dynamics. *Annu. Rev. Phys. Chem.* **1982**, *33*, 223−255.

(5) Moiseyev, N. Quantum Theory of Resonances: Calculating Energies, Widths and Cross-Sections by Complex Scaling. *Phys. Rep.* **1998**, *302*, 212−293.

(6) Moiseyev, N. *Non-Hermitian Quantum Mechanics*; Cambridge University Press, 2011.

(7) Aguilar, J.; Combes, J. M. A Class of Analytic Perturbations for One-Body Schrödinger Hamiltonians. *Commun. Math. Phys.* **1971**, *22*, 269−279.

(8) Riss, U. V.; Meyer, H.-D. Calculation of Resonance Energies and Widths Using the Complex Absorbing Potential Method. *J. Phys. B* **1993**, *26*, 4503−4536.

(9) Santra, R.; Cederbaum, L. S. Non-Hermitian Electronic Theory and Applications to Clusters. *Phys. Rep.* **2002**, *368*, 1−117.

(10) Muga, J. G.; Palao, J. P.; Navarro, B.; Egusquiza, I. L. Complex Absorbing Potentials. *Phys. Rep.* **2004**, *395*, 357−426.

(11) Lipkin, N.; Moiseyev, N.; Brändas, E. Resonances by the Exterior-Scaling Method within the Framework of the Finite-Basis-Set Approximation. *Phys. Rev. A* **1989**, *40*, 549−553.

(12) McCurdy, C. W.; Rescigno, T. N.; Byrum, D. Making Complex Scaling Work for Long-Range Potentials. *Phys. Rev. A* **1997**, *56*, 1958−1969.

(13) Riss, U. V.; Meyer, H.-D. Reflection-Free Complex Absorbing Potentials. *J. Phys. B* **1995**, *28*, 1475−1493.

(14) Santra, R.; Cederbaum, L. S. Complex Absorbing Potentials in the Framework of Electron Propagator Theory. I. General Formalism. *J. Chem. Phys.* **2002**, *117*, 5511−5521.

(15) Riss, U. V.; Meyer, H.-D. The Transformative Complex Absorbing Potential Method: A Bridge between Complex Absorbing Potentials and Smooth Exterior Scaling. *J. Phys. B* **1998**, *31*, 2279−2304.

(16) Kosloff, R.; Kosloff, D. Absorbing Boundaries for Wave Propagation Problems. *J. Comput. Phys.* **1986**, *63*, 363−376.

(17) Ghosh, A.; Vaval, N.; Pal, S. Equation-of-Motion Coupled-Cluster Method for the Study of Shape Resonances. *J. Chem. Phys.* **2012**, *136*, 234110.

(18) Zhou, Y.; Ernzerhof, M. Calculating the Lifetimes of Metastable States with Complex Density Functional Theory. *J. Phys. Chem. Lett.* **2012**, *3*, 1916−1920.

(19) Ehara, M.; Sommerfeld, T. CAP/SAC-CI Method for Calculating Resonance States of Metastable Anions. *Chem. Phys. Lett.* **2012**, *537*, 107−112.

(20) Bravaya, K. B.; Zuev, D.; Epifanovsky, E.; Krylov, A. I. Complex-Scaled Equation-of-Motion Coupled-Cluster Method with Single and Double Substitutions for Autoionizing Excited States: Theory, Implementation, and Examples. *J. Chem. Phys.* **2013**, *138*, 124106.

(21) Epifanovsky, E.; Wormit, M.; Kuś, T.; Landau, A.; Zuev, D.; Khistyaev, K.; Manohar, P.; Kaliman, I.; Dreuw, A.; Krylov, A. I. New Implementation of High-Level Correlated Methods Using a General Block-Tensor Library for High-Performance Electronic Structure Calculations. *J. Comput. Chem.* **2013**, *34*, 2293−2309.

(22) Shao, Y.; Fusti-Molnar, L.; Jung, Y.; Kussmann, J.; Ochsenfeld, C.; Brown, S.; Gilbert, A. T. B.; Slipchenko, L. V.; Levchenko, S. V.; O'Neill, D. P.; et al. Advances in Methods and Algorithms in a Modern Quantum Chemistry Program Package. *Phys. Chem. Chem. Phys.* **2006**, *8*, 3172−3191.

(23) Moiseyev, N.; Certain, P. R.; Weinhold, F. Resonance Properties of Complex-Rotated Hamiltonians. *Mol. Phys.* **1978**, *36*, 1613−1630.

(24) Krylov, A. I. Equation-of-Motion Coupled-Cluster Methods for Open-Shell and Electronically Excited Species: The Hitchhiker's Guide to Fock Space. *Annu. Rev. Phys. Chem.* **2008**, *59*, 433−462.

(25) Feng, X.; Luzanov, A. V.; Krylov, A. I. Fission of Entangled Spins: An Electronic Structure Perspective. *J. Phys. Chem. Lett.* **2013**, *4*, 3845−3852.

(26) Sommerfeld, T.; Meyer, H.-D. Computing the Energy-Dependent Width of Temporary Anions from L^2 ab initio Methods. *J. Phys. B* **2002**, *35*, 1841−1863.